Design and Fabrication of a 2-Port Multiple Antenna System for mmWave Application

Priyadarshini K. Desai * and Bindu S.

Department of ECE, B.N.M. Institute of Technology, Bangalore, Karnataka, India; Email: bindu.ct@gmail.com (B.S.)
*Correspondence: priyadarshini.p.r@gmail.com (P.K.D.)

***Abstract*—The next-generation wireless communication technology heading towards the mmWave band requires multiple antenna systems to achieve high diversity, high data rates, and reliability. The design of multiple antenna systems is always associated with the problem of mutual coupling between antenna elements. In order to achieve better system performance, the mutual coupling between the elements has to be minimized. This work basically aims to minimize the mutual interaction among the antenna elements. A 2-port multiple antenna system is presented, with the defected ground structure as a decoupling technique, in order to minimize the mutual coupling. The single microstrip patch antenna is initially designed to operate at 24 GHz; later, it is transformed into a 2-port multiple antenna system. The transformed 2-port multiple antenna is loaded with the defective ground structure. The designed antenna system is fabricated, and practical measurements are carried out. The isolation achieved with defective ground structure through simulation is –27dB, and the practical measured value is –40dB. The 2-port multiple antenna system performance is assessed through the following metrics: Envelope Correlation Coefficient(ECC), Diversity Gain(DG), and Channel Capacity Loss(CCL). For the proposed 2-port multiple antenna the obtained values of ECC, DG and CLL are 0.004, 9.99dB and 0.4 bit/s/Hz. The results of the simulated structure are in good agreement with the fabricated structure. The result shows that defective ground is the better technique to achieve isolation between the closely placed antennas. The defective ground structure is the simplest technique in comparison with other techniques, such as metamaterial, energy band gap etc. The major novelty of the work includes, the design of a 2-port multiple antenna system with single slot and achieving the isolation more than –47dB without affecting the antenna resonating frequency.**

***Keywords*—Microstrip rectangular patch antenna, mmWave band, multiple antenna system, defective ground structure**

I. Introduction

Wireless communication technologies have evolved from the1G to the current 4GLTE. Every generation has provided a better quality of communication in terms of connectivity, data rate, and latency. The improvement is achieved due to changes in the operating frequency and the design of new systems that are able to operate at the required frequency. The fifth-generation wireless communication technology promises to offer a high data rate, that is measured in gigabits per second.

A small cell base station loaded with multiple antennas operating at mm-wave frequency promises to meet the next generation requirements. The multiple antenna systems implementation improves the data rate and small cell implementation results in seamless connectivity.

In any wireless communication system, antenna is one of the crucial component. The antenna dimension is measured in terms of wavelength. If the small base station is designed to operate at mm-wave frequency, then the antenna size reduces drastically. Thus, there has been surge in interest to design antennas operating at mm-wave frequency [1].

The mm-wave communication though offers high bandwidth, it also possesses certain signal attenuation challenges. The information signal gets attenuated at a faster rate when transmitted at mm-wave frequency. This attenuation of the signal is due to various losses such as free-space loss, atmospheric loss, foliage loss, etc. The design of a single omnidirectional antenna will not be sufficient to combat these losses. In order to overcome these losses, single antenna has to be transformed into multiple antenna system.

In multiple antenna systems, antennas are closely placed. These closely placed antennas exhibit very high mutual interaction. The mutual interaction among the antennas leads to the degradation of the multiple antenna system performance. Thus there is a need to increase the isolation between closely placed antennas, in order to improve system performance.

The techniques that are used to increase isolation between antenna elements include defected ground structure, metamaterial, parasitic elements, energy band gap structure etc. Among these techniques, the defected ground structure, is simple, as no additional structure is required to be designed and loaded. The Defective ground structure basically involves introducing a slot in a ground plane of microstrip patch antenna system.

In this work, a 2-port multiple antenna system loaded with defective ground structure is designed and analyzed. Initially, the single antenna resonating at 24GHz is designed and later it is transformed into a 2-port antenna system. The 2-port multiple antenna system is placed on the single substrate and loaded with defective ground structure. A rectangular slot is introduced in the ground plane of 2-port multiple antenna system. The performance analysis of a 2-port multiple antenna with and defective

Manuscript received June 6, 2023; revised July 12, 2023; accepted July 17, 2023.

ground structure is carried out. In the results obtained, it is observed that the antenna operating frequency is not affected by the introduction of rectangular slot in ground plane. Thus, the 2-port system can be transformed into N-port system also.

II. Literature Review

Basically, in the design of the patch antenna, the dielectric substrate plays a very important role when an antenna is intended for high-frequency applications. In [2], the impact of dielectric material on the antenna's performance operating at mmWave frequency is examined. The obtained results show that Rogger 5880 is a more appropriate material to be used when operating at mm-wave frequency. The microstrip patch antenna is designed to operate in Ultra-wideband (UWB), and bandwidth enhancement is achieved by changing its shape [3]. The planned antenna is transformed to 2×2 MIMO, and the decoupling structure is a meta-surface composed of Split Ring Resonator SRR. The measurement shows a transmission coefficient of −43 dB. Envelope Correlation Coefficient ECC and diversity gain are, respectively, 10dB and 0.07. The findings demonstrated that, at UWB frequencies, the use of metamaterials increased the isolation between radiating elements

A unique metamaterial absorber in the form of a flower has been created and is being used as a decoupling structure [4]. The 5.5 GHz WiMAX spectrum is intended for MIMO antenna technology. A metamaterial absorber with a four-element array is intended to form a line between two radiating elements. A −33dB isolation has been attained. ECC, DG, and TARC were the Multiple Antenna performance metrics that were assessed. The obtained ECC and DG values are 0.004 and 10 dB, respectively; however, the radiation efficiency was 68.03%. Due to the partial ground structure, the radiation efficiency is reduced.

For the purpose of reducing mutual coupling in multiple antenna systems, a meta surface antenna array decoupling technique is used [5]. A two-element MIMO antenna array is suspended by a meta-surface composed of SRR with a 5.8 GHz frequency configuration. At the desired frequency band, isolation is −27dB. The ECC obtained is 0.08. By using a hybrid electric and magnetic coupling structure, the isolation in MIMO antenna systems is improved [6]. The operating range of the MIMO antenna system is 2.3–2.8 GHz. A split-ring resonator is a structure that uncouples the radiating element. With a split-ring structure, a −30 dB decoupling factor was achieved. From 2.3 GHz to 2.9 GHz, the ECC is less than 0.005, which is extremely modest. The MIMO antenna's channel capacity loss, which ranges from 1.28 to 16.55 bps/Hz, is also assessed. The sub-6 GHz frequency spectrum is the intended range for the MIMO system.

Broadband SCS for broadcasting and communications applications is built with a quad-band antenna with high isolation MIMO [7]. The quad-band was produced by the dual PIFA and the addition of a self-complementary structure. The developed antenna exhibits good impedance matching at WLAN at 2.4 GHz and 5.15 GHz, L-band, and UHF. First, the antennas were oriented so that they were orthogonally aligned. Next, a connecting line was utilized near the feed point, which essentially served as a band-stop filter at 2 GHz. Finally, a connecting plane is used on the bottom side of the antenna. For an antenna operating at three separate frequencies, all three approaches were utilized. The achieved isolation of the antenna elements is −30dB.

An extremely small MIMO antenna system for WiMAX and WLAN has been designed and investigated [8]. Its radiating elements were arranged orthogonally. A Y-shaped parasitic element is employed between the orthogonal elements in addition to orientation. The system is 20mm by 20mm in size. With 80% radiation efficiency, the transmission coefficient is −43dB, and the ECC is roughly 0.004.

According to a survey [9] on massive MIMO's ability to support the next generation of wireless communication technology, some of its advantages include a ten-fold increase in capacity and a concomitant 100-fold increase in radiated energy efficiency. It is said that the adoption of a significant number of antennas will enable a huge gain in energy efficiency.

A unique decoupling structure is created using the phase shift concept [10]. A shorting pin and a half-wave microstrip line make up the innovative construction. Due to the provision of an additional signal line, the mutual coupling between the nearby patch antennas is minimised. A 7–8dB improvement in isolation exists between the two patch elements at 3.16 GHz, the frequency of operation.

When employed in antenna design, the notion of characteristic modes is used to examine the behaviour of a defective ground structure [11]. A methodical process is used to conduct the analysis and determine whether or not the isolation may be improved. Two 4-element and one 2-element MIMO antenna systems with individual monopole and Planar Inverted-F Antenna PIFA elements were constructed for the case study. The paper came to the conclusion that an 11 dB isolation increase is possible with the addition of Defected Ground Structure DGS.

Two other types of feed lines, one based on a substrate-integrated cavity and the other on surface plasmon polarization, are also used to improve isolation [12]. Broadband decoupling is made possible by the SIW and SSP's high-pass and low-pass feeding networks. A T-junction power combiner/divider is designed to excite a 2-element array [13]. To increase isolation, defective earth with shapes like rectangles, circles, and zigzags is inserted into the soil. The designed antenna operates in the 25.5–29.6 GHz mm-Wave band. 8.3dB is the peak gain obtained. For the designed MIMO antenna with a varied DGS structure, ECC, MEG, and DG are estimated.

For use with UWB, a single negative metamaterial monopole antenna is created [14]. The SNG metamaterial is put into the single-monopole antenna. By increasing the bandwidth from 3.08 GHz to 14.1 GHz, an average gain of 4.54dB was provided. An antenna is used as the microwave oven's temperature sensor [15]. The sensor node, which serves as a temperature-detecting element, is

where the UWB antenna is mounted. The resonance frequencies for metamaterial are 250 MHz, 200 MHz, 150 MHz, and 50 MHz [16]. The main function of metamaterials is to act as sensors to detect different chemical samples that have a strong dielectric response

Metamaterial is employed as the superstrate in a split-ring resonator [17]. When a patch antenna is loaded with superstrate, the gain increases by 7.6dB at 5.9 GHz, but the bandwidth remains unchanged. Gain with metamaterial as a substrate is the antenna parameter that has been improved. The gain enhancement using two layers of meta-surfaces at 28 GHz is discussed in [18]. The gain is increased by 2 dB with the addition of the superstrate layer. For the positioning of the layer, there are no predefined rules

A superstrate that uses a split-ring resonator at UWB frequency has been developed [19]. The analysis of a split-ring resonator with more rings and more space between them has been done. The increase in bandwidth is demonstrated by the patch antenna with a loaded SRR substrate. Exclusive investigation of the s-band and x-band gap-linked hexagonal split ring resonator metamaterial [20]. The 10mmx10mm GCHSRR is printed on the dielectric material FR-4. The developed metamaterial displayed negative permittivity and permeability in the S- and X-band spectra. At 4.27 GHz, 5.42 GHz, and 12.40 GHz, the metamaterial's absorption peaks were found to be 99%, 98%, and 82%, respectively. The proposed GCHSRR is appropriate for microwave applications due to its strong field absorption quality.

At 15 GHz, a brand-new single negative metamaterial made up of concentric rings and crossing lines is designed [21]. At several frequency bands, the developed metamaterial exhibited a single negative behavior. The patch is positioned below the metamaterial. With the introduction of metamaterial into the ground plane, an increase in bandwidth and impedance matching is seen from 2 GHz to 20 GHz.

A 3-port multimode antenna is used as a unit element in the design and analysis of a small, 108-element base station antenna array [22]. The 75mmx75mmx14.8mm three-layer with aperture couple feed made up the three-port multimode antenna. The middle patch is a square ring patch and is connected to ports 1 and 2. The gain obtained through the unit element is 6.5dB, and the impedance bandwidth is 254 MHz (2.248 GHz–2.486 GHz) and 238 MHz (2.248 GHz–2.486 GHz) when ports 1 and 2 are excited. The upper patch is a square patch with a slot and is connected to port 3. The elements' mutual coupling is kept at −14dB.

Microstrip patch antennas are integrated with metamaterial to improve their functionality [23]. To increase the impedance bandwidth, the patch is loaded with a complementary split-ring resonator structure close to the feedline. The CSRR in the ground structure, which also had a flaw, was bigger in size than the CSRR that had been loaded with the patch. The entire building is made to function at the 2.4 GHz Wi-Fi frequency.

A 1.7789 GHz and 2.459 GHz dual-band terahertz metamaterial absorption device is created [24]. A metallic mirror and two similar square patches make up the absorption device. There is an insulating material positioned between the patch and the metallic mirror. It is possible to realize two resonance peaks with almost complete absorption. Different field creation techniques resulted in a Q-factor of 6.9156 and an ultra-high Q-factor of 296.28 is being achieved.

A millimetre-Wave energy bandgap structure is intended to function [25]. A conventional uniplanar EBG unit cell is transformed into an EGB unit cell by adding two connecting bridges and etching two slots. The EBG's size is 78% smaller than a typical unit. The massive antenna array at 60 GHz millimetre wave frequency can use the planned EGB's performance as a decoupling device.

III. Proposed Mulitple Antenna System Design and Analysis

In this manuscript, a 2-port Multiple antenna system is designed. Initially, a single microstrip patch antenna is designed to resonate at 24 GHz; the details are discussed in Section A. CST microwave studio is used to design and simulate the multiple antennas, followed by ABviewer-15 to verify the .dxf file extracted from CST for fabrication. Section B gives an introduction to the performance metrics that are used in multiple antenna system assessment. The microstrip patch antenna is converted into a 2-port Multiple antenna system. The slot is introduced in the ground plane of the antenna system, and the detailed analysis is explained in Section C.

A. Microstrip Rectangular Patch Antenna Design and Analysis

A dielectric substance is often placed between the two metallic patches in a microstrip patch antenna. The radiating patch is the metallic patch that is located beneath the substrate. The substrate typically has a dimension of λ/2. When working at a higher frequency, a dielectric material is chosen that has a low loss in the substrate. The Rogger 5880 substrate is chosen because it has a relative permittivity of 2.2 and a thickness of 0.5mm, and it is intended to work at 24GHz. The Eqs. (1–5) are used to compute the patch antenna's physical parameters.

$$W_{patch} = \frac{c}{2f_0\sqrt{\frac{\varepsilon_r+1}{2}}} \tag{1}$$

$$L_{patch} = L_{eff} - 2\Delta L \tag{2}$$

$$\Delta L = 0.412t_s \frac{(\varepsilon_{eff}+0.3)(\frac{W}{t_s}+0.264)}{(\varepsilon_{eff}-0.258)(\frac{W}{t_s}+0.8)} \tag{3}$$

$$L_{eff} = \frac{C}{2f_0\sqrt{\varepsilon_{eff}}} \tag{4}$$

$$\varepsilon_{eff} = \frac{\varepsilon_r+1}{2} + \frac{\varepsilon_r-1}{2}[1+12\frac{t_s}{W}]^{-1/2} \tag{5}$$

Using the aforementioned calculation, the microstrip patch antenna's dimensions are Wp= 4.2mm and Lp= 4.1mm. The antenna is designed to have an optimal length

and width so that it can resonate at the necessary frequency of 24GHz. The attachment of the antenna to its feed line is crucial since a microstrip line is employed as the feed line. According to Eq. (6), the microstrip line's characteristic impedance is dependent on the line's height, width, and permittivity

$$Z_c = \frac{120\pi}{\sqrt{\varepsilon_{eff}}\left[\frac{W_f}{t_s} + 1.393 + 0.667\ln\left(\frac{W_f}{t_s} + 1.44\right)\right]} \quad (6)$$

with ts standing for the height of the dielectric substrate, Wf for the line's width, and εeff for the substrate's effective permittivity. To achieve adequate impedance matching, the feed width is parametrically changed. A 0.5mm feed width is used to provide better impedance matching. Table I displays the single microstrip patch antenna's dimensions.

TABLE I. DIMENSIONS OF MICROSTRIP RECTANGULAR PATCH ANTENNA

MRPA Structure	Parameter (Symbol)	Value (mm)
Copper Ground	Length (LG)	15
	Width (WG)	15
	Thickness (tG)	0.017
Dielectric Material	Substrate_Width (Ws)	15
	Substrate_Length (Ls)	15
	Substrate_Thickness(ts)	0.5
Rectangular Metal Patch	Patch_Width (Ws)	4.74
	Patch_Length (Lp)	3.84
	Patch_Thickness (t_p)	0.017

B. *Performance Metrics for Evaluation of Multiple Antenna Systems*

The performance of the Multiple Antenna System can be evaluated using a variety of metrics [7]; in this work, the envelope correlation coefficient (ECC), Diversity Gain (DG), and Mean Effective Gain (MEG) are used to assess the performance of the proposed multiple antenna system. In a multiple antenna system, the radiating elements must be highly isolated; ECC measures the correlation between the radiating elements. The Correlation is observed both in terms of Field pattern and S-parameters. ECC has been assessed in this work employing Eq. (7) (where i and j are antennas and N is the total number of antennas taken under consideration) via S-parameters between components of the shown Multiple Antenna system.

$$\rho_e = \frac{\left|\sum_{n=1}^{N} S_{i,n}^{*} S_{n,j}\right|^2}{\prod_{k=(i,j)} 1 - \sum_{n=1}^{N} S_{i,n}^{*} S_{n,k}} \quad (7)$$

To satisfy the power standards, the Mean Effective Gain (MEG) of any two antennas in a Multiple Antenna System must be –3dB. The incident average power to antenna average received power ratio is known as MEG. The power differential over a channel or propagation medium is assessed or evaluated by a multiple antenna system's mean effective gain. It is a vital metric for determining how well a multiple antenna system works. The MEG computation is carried out using Eq. (8).

$$MEG = \int_0^{2\pi}\int_0^{\pi}\left[\frac{XPR}{1+XPR}G_\theta(\theta,\varphi)P_\theta(\theta,\varphi) + \frac{XPR}{1+XPR}G_\theta(\theta,\varphi)P_\theta(\theta,\varphi)\right] sin\theta\, d\theta\, d\varphi \quad (8)$$

Gφ and Gθ are the power gain patterns of the antenna when θ is varied, and φ is constant in the case of Gφ and vice versa Gθ. XPR=0 for an outdoor uniform propagation environment. Diversity Gain describes the degree to which Multiple Antenna System outperforms SISO (Single Input Single Output). It can be calculated using relation 9. When using maximum-ratio combining, the maximum diversity gain is 10 at the 1% probability level, and ep is the diversity gain reduction factor resulting from the signal correlation between the two antennas (e is the envelope correlation coefficient).

$$DG = 10 \times e_p = \sqrt{(1 - |0.99e\rho_{ij}|)^2} \quad (9)$$

TARC is an important parameter to characterize multiple antenna system frequency bandwidth and radiation performance under the diverse nature of multiple antennas. It signifies the importance of impedance bandwidth and non-varying resonance frequency even when the input signal phase θ changes for all the input ports. A generalized equation of TARC has been defined for multiple-port antenna combining all scattering parameters when the antenna is linearly polarized after considering the TARC formulation given in Eq. (10)

$$TARC = \frac{\sqrt{\sum_{i=1}^{N}\left|S_{i1} + \sum_{m=2}^{N} S_{im} e^{j\theta m-1}\right|^2}}{\sqrt{N}} \quad (10)$$

CCL is one of the vital diversity performance check-up parameters for multiple antennas. CCL helps in signifying the maximum attainable limit of message transmission rate up to which signal can be transmitted continuously over the communication channel with a loss of fewer than 0.4 bits/s/Hz over the operating frequency range. It can be computed using the following Eq. (11):

$$C_{loss} = -\log_2 det(\alpha^R) \quad (11)$$

where $\alpha^R = \begin{bmatrix} \alpha_{11} & \alpha_{12} & \alpha_{13} \\ \alpha_{21} & \alpha_{22} & \alpha_{23} \\ \alpha_{31} & \alpha_{32} & \alpha_{33} \end{bmatrix}$

where $\alpha_{ii} = 1 - \sum_{j=1}^{N}\left|S_{ij}\right|^2$ and $\alpha_{ij} = -\left(S_{ii}^{*} S_{ij} + S_{ji}^{*} S_{ij}\right)$

C. *Design of 2-Port Multiple Antenna with a Slotted Ground Structure Study.*

The intended microstrip patch is often transformed into a 2-port Multiple Antenna System. Fig. 1 depicts the top and bottom views of a 2-port Multiple Antenna System with a slotted ground construction. The 2×2 antennas are linearly oriented. The dimension of the 2-port multiple antenna is 15mm × 15mm×0.508mm. The distance between the antenna is λ/2, where λ is the free space wavelength. The slot having a dimension of 2 mm × 12

mm (x, y), is introduced in the ground plane. The current flow is typically interrupted when a slot is introduced, increasing the isolation between the radiating elements, thereby minimizing mutual coupling.

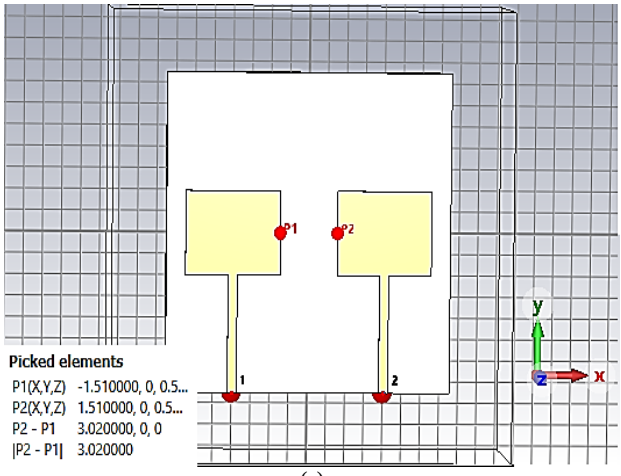

(a)

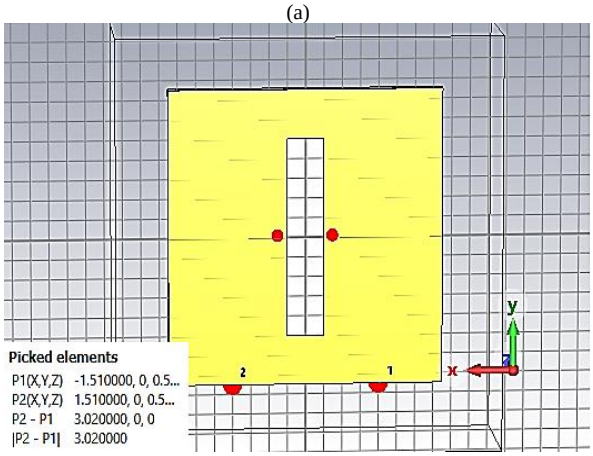

(b)

Figure 1. A 2-port Multiple Antenna System with Slotted Ground (a)Top view (b) Bottom view

Due to the introduction of slot in the ground, there will discontinuity in the fields and surface current. The surface current interaction depicted in Fig. 2 shows reduced interaction among the antenna elements. As a result, the isolation between the parts grows, improving the performance of the multiple antenna system. The Fig. 3 indicates the transmission and radiation efficiency of the multiple antenna system is above 95%.

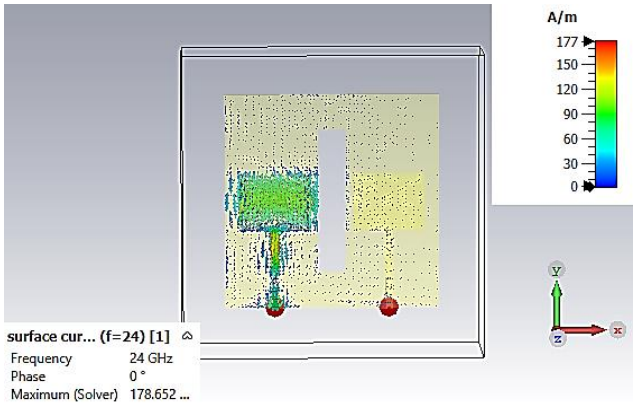

(a)

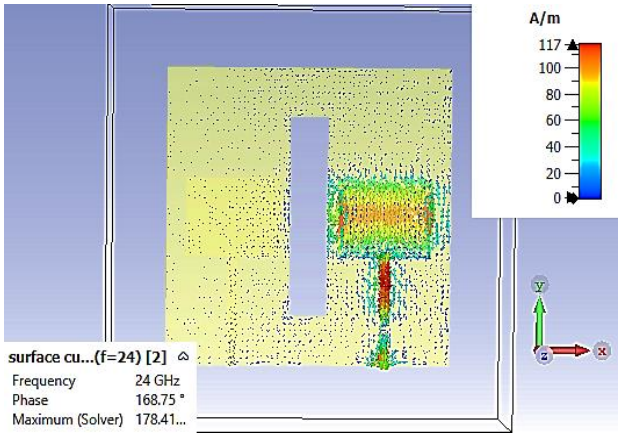

(b)

Figure 2. Surface current density of 2-port multiple antenna system with slotted ground structure (a). Antenna-1 Excited (b.) Antenna-2 Excited.

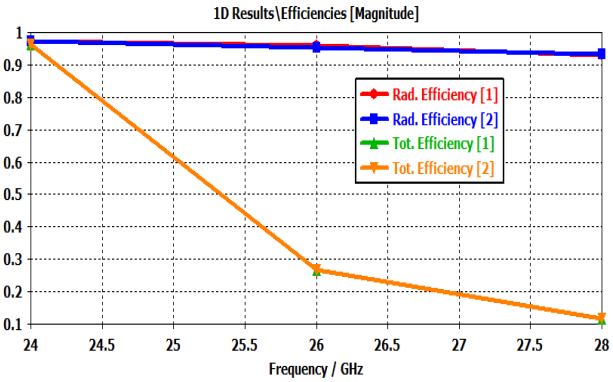

Figure 3. Efficiency of 2-port multiple antenna system with slotted ground structure.

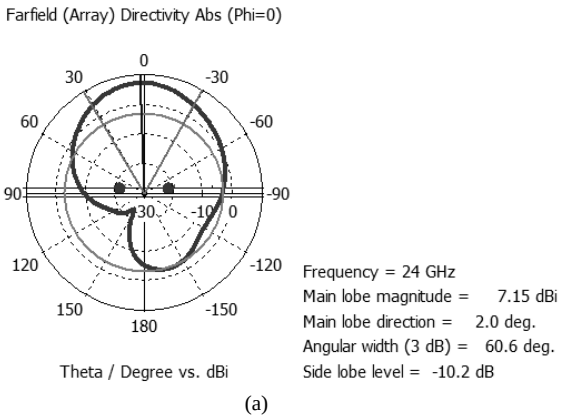

(a)

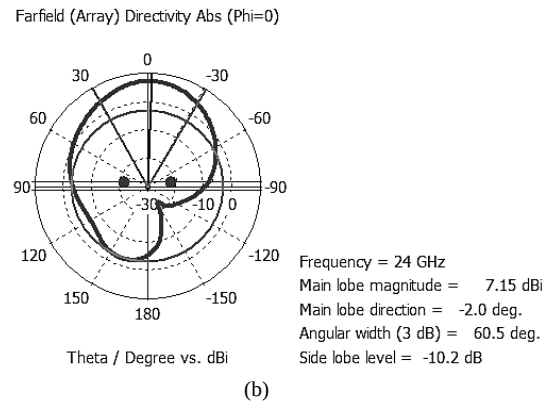

(b)

Figure 4. E-plane pattern of (a) Antenna-1 (b) Antenna-2.

In the E-plane pattern of main lobe of antenna 1 is at 20 and antenna-2 is at −20, indicating pattern diversity as observed from Fig. 4. The 3dB angular width of both the radiating elements is around 60.60 with side lobe level of −10.2dB

D. *Fabrication of 2-port Multiple Antenna System with Defective Ground Structure*

The 2-port multiple antenna system is fabricated on a Rogger 5880 with 15mm × 15 mm × 0.508mm dimensions. The thickness of the copper metal is 0.017mm. Fig. 5 shows the fabricated 2-port multiple antenna system. The figure indicates the top view, and in the bottom view, a ground with a slot of 2 × 10 (mm^2) dimension can be observed.

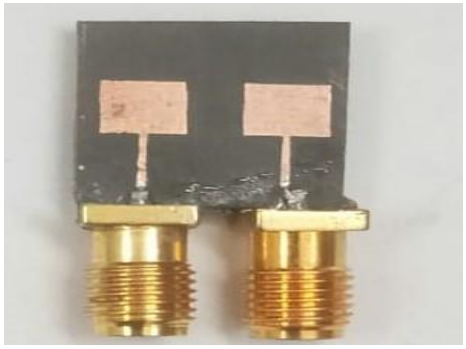

(a)

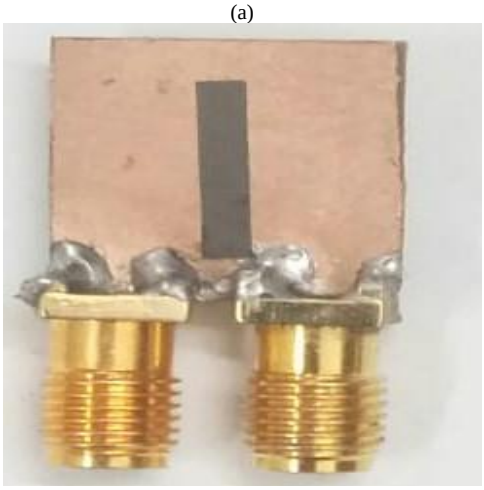

(b)

Figure 5. Fabricated 2-port multiple antenna system (a). Top view (b). Bottom view

The measurement of the reflection coefficient and transmission coefficient is carried out using Agilent N5247A: A.09.90.02.

IV. Result and Discussion

Fig. 6 shows the Network Analyzer Agilent N5247A: A.09.90.02, where the s-parameter measurement of a fabricated antenna is carried out. Due to the placement of connectors in close proximity, a shift in frequency of about 2 MHz is observed during the measurement. The return loss S11 of −35dB is observed at 23.876 GHz, and the return loss S22 is −25dB at 24.22 GHz.

Figure 6. Experimental setup for the measurement of S-parameter of Fabricated 2-port Multiple Antenna

The antenna-2 exhibits multi-band features, including 24 GHz. Figs. 7 (a) and (b) indicate that the simulated results are in good agreement with the measured results. The transmission coefficients obtained are −27dB and −45 dB with the introduction of the ground slot.

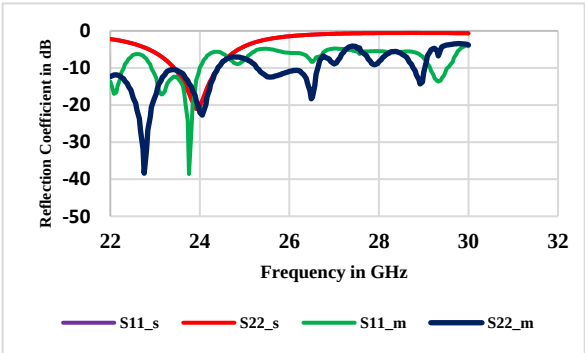

(a)

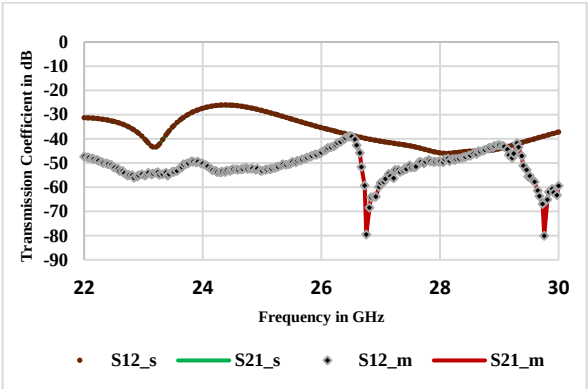

(b)

Figure 7. The Plot of fabricated and simulated (a). Reflection coefficient (b) Transmission coefficient.

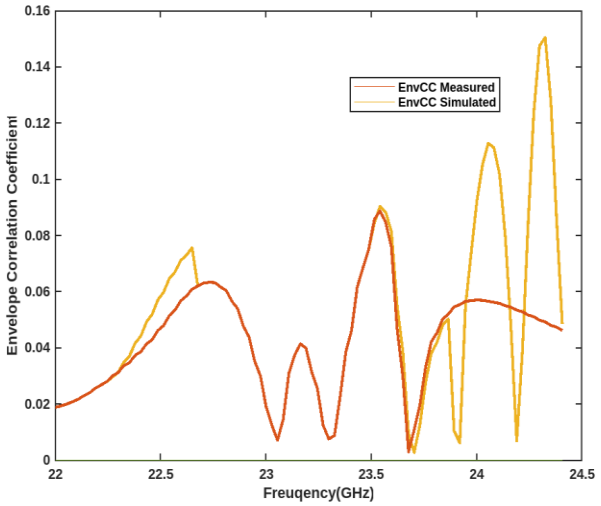

Figure 8. ECC of 2-port multiple antenna system.

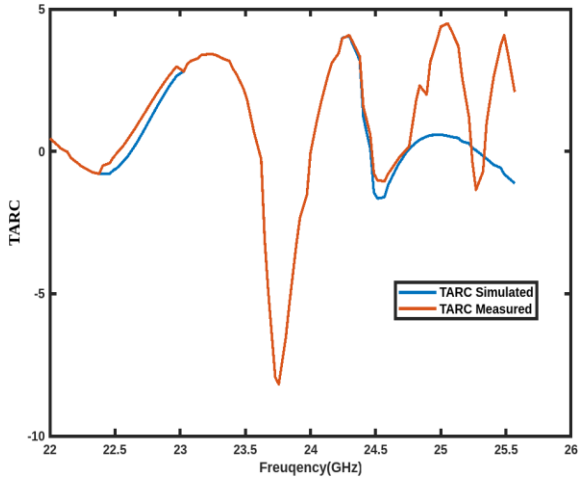

Figure 9. TARC of 2-port multiple antenna system.

The results obtained clearly indicate that with the introduction of single slots, there is an increase in the isolation between elements. The multiple antenna system performance metrics are evaluated for both simulated and fabricated 2-port multiple antenna systems. The three performance metrics considered to assess the design are ECC, TARC, and CCL. Since the designed antenna offers an efficiency of 97%, ECC evaluation through the s-parameter is considered. Fig. 8 indicates that the ECC is less than 0.05, indicating the antenna offers better isolation with the introduction of the slot in the ground.

The total active reflection coefficient following S11 and S22 of the designed 2-port multiple antenna is indicated in Fig. 9. TARC is below 0 dB for the required frequency. The Channel capacity loss obtained is less than 0.5 bit/s/Hz for both simulated and fabricated 2-port multiple antenna systems, as observed in Fig. 10.

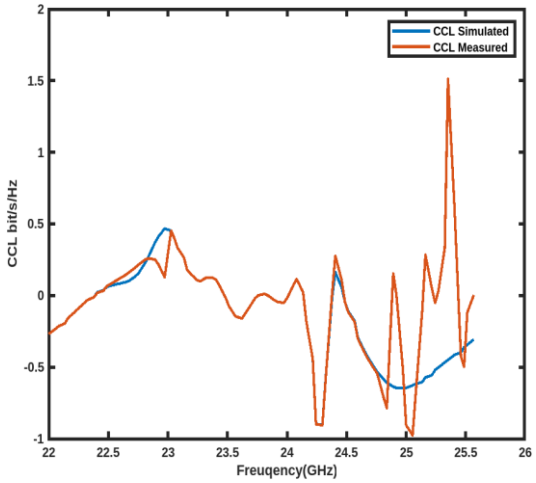

Figure 10. CCL of 2-port multiple antenna system.

The Table II gives a comparison of the earlier work and the proposed work. The earlier proposed work used defected ground structure as decoupling structure to increase the isolation between antenna elements. From Table II, it can be noted that the dimension of 2-port multiple antenna of proposed work is small with isolation greater than –40dB and offering efficiency more than 95%

TABLE II. COMPARISON OF THE PROPOSED WORK WITH LITERATURE

Ref	Frequency (GHz)	Ports	Dimension(mm^3)	Gain (dBi)	Efficiency (%)	Isolation (dB)	ECC
Usman *et al.* [26]	28	2	33 × 27.5	6.9	-	>30	-
Lakrit *et al.* [27]	26.65-29.2	2	26 × 11	5	99.5	>25	<0.002
Wani *et al.* [28]	28	4	30 × 30	6.1	92	29	<0.16
Sharma *et al.* [29]	28	4	48 × 31	10	-	>21	<0.0015
Kamal *et al.* [30]	27.6-28.6; 37.4-38.6	4	20 × 24	7.9	>85	>28	<0.001
Raheel *et al.* [31]	24.10-27.18	4	24 × 20	3	>80	>16	<0.1
Desai *et al.* [32]	25.5-29.6	4	30 × 35	8.3	-	>15	<0.01
Khalid *et al.* [33]	27.5-29.6	4	25 × 15	7.8	95	>17	<0.0001
This Work	24	2	15 × 15	7.28	>95	>40	<0.04

V. Conclusion

The work mainly aims to design a compact 2-port multiple antenna system at mm-wave frequency exhibiting high isolation between the antenna elements. Initially, a single microstrip patch antenna was designed to operate at 24 GHz and later transformed into a 2-port system. The design of a 2-port multiple antenna system is carried out, keeping the substrate dimension at 15 mm × 15 mm × 0.508 mm, which is the same as that of a single patch. There is no change in substrate length or width during the transformation of a single patch into a 2-port antenna system. The major novelty of the work includes the design of a 2-port multiple antenna system with the introduction of a single slot instead of multiple slots. The isolation between antenna elements is more than −40dB, with the introduction of a single slot, with no other increase in the design complexity. Designed multiple antenna system is more compact, with spacing between the elements being 3.01mm Thus, the designed antenna system is a compact 2-port antenna system. Due to the increase in the isolation factor, the assessed multiple antenna performance metrics are in the required range, i.e., ECC is less than 0.05 and CCL is less than 0.5 bit/s/Hz. The designed 2-port antenna system can be transformed into any NxN multiple antenna system. Since the designed system is compact, it can be easily integrated with other electronic devices operating at an mm-Wave frequency and for any mm-Wave application

Conflict of Interest

The authors declare no conflict of interest.

Author Contributions

Priyadarshini K. Desai – Design, Experimentation, Analysis of Results, and Writing the manuscript. Bindu. S. Conceptualization and review of the manuscript. all authors had approved the final version.

Acknowledgment

I want to thank the B.N.M Institute of Technology and Visvesvaraya Technological University for their constant support.

References

[1] D. Muirhead, M. A. Imran, and K. Arshad, "A Survey of the challenges, opportunities, and use of multiple antennas in current and future 5G small cell base stations," *IEEE Access*, vol. 4, pp. 2952–29654, July 2016.

[2] P. K. Desai and S Bindu, "Impact of dielectric substrate on the performance of Microstrip Patch Antenna at millimeter wave frequency," presented at 2023 International Conference on Intelligent and Innovative Technologies in Computing, Electrical and Electronics (IITCEE), BNMIT, Bangalore, Karnataka, India January 27-28, 2023.

[3] H. Sakli, C. Abdelhamid, C. Essid, and N. Sakli, "Metamaterial-based antenna performance enhancement for MIMO system applications," *IEEE Access*, vol. 9, pp. 38546–38556, March 2021.

[4] P. Garg and P. Jain, "Isolation improvement of MIMO antenna using a novel flower-shaped metamaterial absorber at 5.5GHz WiMAX band," *IEEE Trans. Circuits Syst*., vol. 67, pp. 675–679, April 2020.

[5] Z. Wang, L. Zhao, Y. Cai, S. Zheng, and Y. Yin, "A meta-surface antenna array decoupling (MAAD) method for mutual coupling reduction in a MIMO antenna system," *Sci. Rep*., vol. 8, pp. 3152–3159, 2018.

[6] C. D. Xue, X. Y. Zhang, Y. F. Cao, Z. Hou, and C. F. Ding, "MIMO antenna using hybrid electric and magnetic coupling for isolation enhancement," *IEEE Trans. Antennas Propag*., vol 65, pp. 5162–5170, 2017

[7] C. Yang, J. Kim, H. Kim, J. Wee, B. Kim, C. Jung, "Quad-band antenna with high isolation MIMO and broadband SCS for broadcasting and telecommunication services," *IEEE Antennas Wirel. Propag. Lett*., vol. 9, pp. 584–587, Feb 2010.

[8] A. Bhattacharya and B. Roy, "Investigations on an extremely compact MIMO antenna with enhanced isolation and bandwidth," *Microw. Opt. Technol. Lett.*, vol. 62, pp. 845–851, Oct 2019.

[9] E. G. Larsson, O. Edfors, F. Tufvesson, and T. L. Marzetta, "Massive MIMO for next generation wireless systems." IEEE Commun. Mag., vol 52, pp. 186–195, Jan 2014

[10] Pei, T.; Zhu, L.; Wang, J.; Wu, W. "A low-profile decoupling structure for mutual coupling suppression in MIMO patch antenna," *IEEE Trans. Antennas Propag.* , vol. 69, pp. 6145–6153. July 2021.

[11] A. Ghalib and M. S. Sharawi, "TCM analysis of defected ground structures for MIMO antenna designs in mobile terminals," IEEE Access, vol 5, pp. 19680–19692, Sept 2017.

[12] B. C. Pan and T. J. Cui, "Broadband decoupling network for dual-band microstrip patch antennas," *IEEE Trans. Antennas Propag*, vol 65, pp 5595–5598, Aug 2017.

[13] M. Khalid *et al*., "4-port MIMO antenna with defected ground structure for 5G millimeter wave applications," *Electronics*, vol. 9, p. 71, Jan 2020.

[14] S. S. Al-Bawri *et al*., "Compact ultra-wideband monopole antenna loaded with metamaterial," *Sensors*, vol. 20, p. 796, Jan 2020.

[15] J. Yao, F. M. Tchafa, A. Jain, S. Tjuatja, and H. Huang, "Far-feld interrogation of microstrip patch antenna for temperature sensing without electronics*," IEEE Sens. J*., vol. 16, pp. 7053–7060, 2016.

[16] Y. I. Abdulkarim *et al*., "Design and study of a metamaterial based sensor for the application of liquid chemicals detection," *Journal of Material Reseacrh and Technology*, vol. 9, pp. 10291–10304, July 2020.

[17] D. Gangwar, S. Das, and R. L. Yadava, "Gain enhancement of microstrip patch antenna loaded with split ring resonator based relative permeability near zero as superstrate," *Wireless Personal Communications*, vol. 96, pp. 2389–2399, May 2017.

[18] P. K. Desai and S. Bindu, "Design and analysis of microstrip patch antenna properties with split-ring resonator metamaterial as superstrate at mmWave frequency," I*nternational Journal of Scientific Research in Computer Science, Engineering and Information Technology*, vol. 8, pp. 217–224, June 2022.

[19] S. K. Patel, C. Argyropoulos, and Y. P. Kosta, "Broadband compact microstrip patch antenna design loaded by multiple split ring resonator superstrate and substrate," *Waves in Random and Complex Media*, vol. 27, pp. 92–102 June 2016.

[20] M. S. Islam *et al*., "A gap coupled hexagonal split ring resonator based metamaterial for S-band and X-band microwave applications," *IEEE Access*, vol. 8, pp. 68239–68253 April 2020.

[21] A. R. Azeez, T. A. Elwi, and Z. A. A. Al-Hussain, "Design and analysis of a novel concentric rings based crossed lines single negative metamaterial structure," *Eng. Sci. Technol. Int. J*., vol. 20, pp. 1140–1146 June 2017.

[22] A.J ain and S. K. Yadav, "Design and analysis of compact 108 element multimode antenna array for massive MIMO base station," *Prog. Electromagn. Res.*, vol. 61, pp. 179–184, Jan 2016.

[23] G. Geetharamani and T. Aathmanesan, "Design of metamaterial antenna for 2.4 GHz WiFi applications," *Wirel. Pers. Commun.*, vol. 113, pp. 2289–2300, April 2020.

[24] B. X.Wang, Y. He, P. Lou, and W. Xing, "Design of a dual-band terahertz metamaterial absorber using two identical square patches for sensing application," *Nanoscale Adv*., vol. 2, pp. 763–769, Jan 2020.

[25] M. J. Al-Hasan, T. A. Denidni, and A. R. Sebak, "Millimeter-wave compact EBG structure for mutual coupling reduction applications," *IEEE Transactions on Antennas*,vol. 61, pp 4354–4357, May 2013.

[26] M. Usman *et al.*, "A. compact SIW fed dual-port single element annular slot MIMO antenna for 5G mmwave applications," *IEEE Access*, vol. 9, pp. 91995–92002, June 2021

[27] W. Ali, S. Das, H. Medkour, and S. Lakrit, "Planar dual-band 27/39 GHz millimeter-wave MIMO antenna for 5G applications," *Microsyst. Technol*., vol. 27, pp. 283–292 Jan 2021.
[28] Z. Wani, M. P. Abegaonkar, and S. K. Koul, "A 28-GHz antenna for 5G MIMO applications," *Prog. Electromagn. Res. Lett.*, vol 78, pp. 73–79 Aug 2018.
[29] Y. Sharma *et al*., "Three-element MIMO antenna system with pattern and polarization diversity for WLAN applications," I*EEE Antennas Wirel. Propag. Lett.*, vol. 16, pp. 1163–1166, Nov 2016.
[30] M. M. Kamal *et al.*, "Infinity shell shaped mimo antenna array for mm-wave 5G applications," *Electronics*, vol. 10, p.165, Jan 2021.
[31] K. Raheel *et al*., "E-shaped H-slotted dual band mmwave antenna for 5G technology," *Electronics*, vol. 10, p. 1019 April 2021.
[32] A. Desai *et al*., "Compact wideband four element optically transparent MIMO antenna for mm-wave 5G applications," *IEEE Access*, vol. 8, pp. 94206–194217, Oct 2020.
[33] M. Khalid *et al*., "4-Port MIMO antenna with defected ground structure for 5G millimeter wave applications," *Electronic*s, vol 9, p. 71, Jan 2020.

Copyright © 2023 by the authors. This is an open access article distributed under the Creative Commons Attribution License (CC BY-NC-ND 4.0), which permits use, distribution and reproduction in any medium, provided that the article is properly cited, the use is non-commercial and no modifications or adaptations are made.